Analysis of Mineral Nutrients in Biochar Derived from Plants in Mining Areas

Bing Wang,[a] Mengke Cui,[a] Jianghao Wang,[a] Bo Liu,[a] Shuai Wang,[a] Yonggang Li,[b,*] Xiaoqing Jia,[a] Xuan Zhang,[a] Zhiyu Gu,[a] Kenji Ogino,[c] and Yuxian Hu,[a,*]

Phytoremediation is a critical technique for remediating heavy metal-contaminated soils in coal gangue zones of mining areas. However, resource valorization of plant residues after heavy metal remediation poses considerable challenges. Converting these residues into biochar *via* thermochemical routes yields a material enriched with mineral nutrients (*e.g.*, Ca, Mg, Fe, Mn, Cu), conferring potential as a soil amendment. This study focused on remediation plants in coal gangue-affected mining regions, selecting *Artemisia annua* (a typical restoration plant) to prepare biochar through pyrolysis and hydrothermal carbonization (HTC). Inductively coupled plasma mass spectrometry (ICP-MS) was used for quantitative analysis of mineral nutrients, providing a scientific basis for resource valorization of heavy metal-laden biomass residues from mining area remediation plants. The results indicated that, except for slight Mg fluctuation in hydrothermally carbonized biochar relative to the raw material, mineral nutrient concentrations (Ca, Mg, Fe, Mn, Cu, Zn) in biochar prepared under other conditions were significantly enhanced (1.53 to 3.14 times *via* pyrolysis and 1.36 to 2.78 times *via* HTC). Furthermore, mineral nutrient concentrations under certain conditions complied with the Chinese agricultural industry standard for biochar (NY/T 4159-2022).

DOI: 10.15376/biores.21.1.570-579

Keywords: Mine restoration plants; Mineral nutrients; Artemisia annua; Biochar

Contact information: a: School of Environment and Resources, Taiyuan University of Science and Technology, 66 Wa-liu Road, Taiyuan, 030024, Shanxi, China; b: Guangxi Key Laboratory of Urban Water Environment, College of Chemistry and Environmental Engineering, Baise University, Baise 533000, China; c: Graduate School of Bio-Applications and Systems Engineering, Tokyo University of Agriculture and Technology, Koganei, Tokyo 184-8588, Japan;
**Corresponding authors: li.yonggang@126.com; huyuxian@tyust.edu.cn*

INTRODUCTION

By the end of 2024, China had cumulatively restored over 333,300 hectares of legacy abandoned mines, and phytoremediation accounted for 15 to 20% of this area (50,000 to 66,000 hectares). In the Yellow River Basin (Shanxi, Henan, Shaanxi) related research has focused on the treatment of cadmium (Cd) and arsenic (As) pollution. In the Yangtze River Basin (Hunan, Guangdong, Yunnan), studies have focused on the combined pollution of arsenic (As), cadmium (Cd), and mercury (Hg). In the Northeast Region (Liaoning, Jilin), research has mainly focused on the treatment of heavy metals and soil degradation (Shi *et al*. 2022). While phytoremediation technology treats heavy-metal-contaminated soil, it also generates biomass residues with excessive heavy metals. The traditional treatment methods for such heavy-metal-containing biomass residues mainly include incineration, composting, and compression landfill (Song 2023). Incineration is the

most traditional method for treating such biomass residues, but in its actual operation, fly ash is likely to cause pipeline blockage problems (Nong 2023). The composting process has the defects of a long cycle and large equipment investment (Kou 2023). The compression landfill method has a short implementation cycle, but the generated filtrate containing heavy metals has a higher pollution possibility, cannot achieve recycling, and has a relatively high environmental risk (Liu 2025).

As a product of the pyrolysis and HTC of mining area remediation plants (Zhang *et al*. 2023), biochar can achieve metal immobilization. This ability can be attributed to its unique porous structure and surface chemical properties. Its metal immobilization capacity stems from the synergistic effect of physical adsorption and chemical passivation: a large number of microporous structures intercept metal ions through pore filling, and the surface oxygen-containing functional groups can form stable complexes with metal ions (Xing 2021). However, this does not mean that metal elements are completely non-leachable from biochar (Li *et al*. 2023); instead, it significantly reduces their environmental mobility and bioavailability through physical barrier and chemical binding, making this immobilization effect relative and condition-dependent (Tao *et al*. 2023). For soil amendment, biochar can enhance the porosity and water-holding capacity of barren soils in mining areas (Li *et al*. 2018). The mineral ions (*i.e.* nutrients) that it contains can be gradually released, thereby increasing soil organic matter content. Additionally, by regulating the microenvironment, the biochar can promote the abundance of functional microbial communities such as nitrogen-fixing bacteria and phosphate-solubilizing bacteria, accelerating nutrient cycling and pollutant degradation (Zhang *et al*. 2010).

Recently, research on biochar has mainly focused on biochar modification, while little research has been done on converting mining area phytoremediation plants into mineral nutrient-rich biochar *via* thermochemical routes. In this study, two preparation processes (pyrolysis and HTC) were adopted to produce *Artemisia annua* biochar under six temperature gradients. ICP-MS was utilized for the quantitative analysis of mineral nutrients in the biochar prepared under different conditions. The study aimed to investigate the effects of preparation parameters (*e.g.*, temperature and heating rate) on the characteristics of mineral nutrients during the biochar production from *A. annua* (a typical heavy metal phytoremediation plant in mining areas). These findings provide a theoretical basis for producing mineral nutrient-rich biochar from biomass residues of mining area heavy metal phytoremediation plants, thus offering a novel technical approach for the safe and efficient utilization of such plant residues.

EXPERIMENTAL

Collection and Processing of Materials

The sampling area was set in a coal gangue pile of a mining area in Jincheng City, Shanxi Province, China. Cinnamon-like soil is the dominant soil type in the mining area, with parent materials mainly including loess-like materials, weathered sandstone, and weathered limestone (Wang 2019). Leaching and coal gangue pile dust from the coal gangue pile area have resulted in cumulative pollution of Cd, Cr, Cu, Mn, and Ni in the soil of the mining area and its surrounding regions to varying degrees.

Artemisia annua is a commonly used plant for heavy metal remediation in the coal gangue area of the local mining district, and it is also a pioneer and dominant species of herbaceous plant communities in different vegetation types (Liu *et al*. 2020). Collected

from this area, the *A. annua* samples were washed thoroughly, cut into small pieces, rinsed with deionized water, and air-dried naturally. They were then dried in a constant-temperature oven at 70 °C for 24 h, crushed, and sieved through a 65-mesh sieve (250±9.9 μm).

Preparation of Mineral Nutrient-Rich Biochar

Preparation of biochar by pyrolysis

A total of 5 g of the treated *A. annua* samples was placed in a quartz crucible. The pyrolysis temperatures were set at 400, 500, and 600 °C, with a heating rate of 5 °C/min. Pyrolysis was conducted for 2 h under a N_2 flow of 100 mL/min in a high-temperature tube furnace to prepare biochar. After pyrolysis, the biochar was washed with deionized water, dried, and stored in bags.

Preparation of biochar by HTC

A total of 5 g of the treated *A. annua* samples was placed into a high-pressure reactor. The HTC temperatures were set at 220, 240, and 260 °C, with a solid-to-liquid ratio of 1:10 (g/mL). The temperature was maintained for 4 h, and the reaction pressure was automatically sustained. The reactor was allowed to cool naturally to room temperature. After washing with deionized water and drying, the samples were stored in bags.

Performance Characterization

The *A. annua* samples were weighed, and the 6 biochar samples of 0.2 g each (accurate to 0.0001 g) were prepared in the digestion tank. After adding 5 mL of HNO_3, 3 mL of HCl, and 2 mL of HF, microwave digestion was performed. The temperature was set in three stages: 150, 180, and 210 °C, with each heating stage lasting 6 min and holding times of 10 min, 15 min, and 15 min for complete digestion. After the digestion system cooled to room temperature, the acid was removed in a fume hood until approximately 1 mL remained. The solution was transferred to a 25 mL volumetric flask, diluted to volume with ultrapure water, filtered through a 0.45 μm microfiltration membrane, shaken thoroughly, and then detected by ICP-MS. Blank controls and certified reference materials were implemented for quality control, with 3 parallel samples prepared during the determination.

RESULTS AND DISCUSSION

Analysis of Types and Concentrations of Raw Mineral Nutrients

As shown in Fig. 1 (a-b), *A. annua* was found to contain various mineral nutrient elements. Among macro-mineral elements, the content of Ca was up to 13200 $mg \cdot kg^{-1}$, and that of Mg was 2470 $mg \cdot kg^{-1}$. Both of these are core nutrients for plant growth. For micro-mineral elements, the content of Fe is 1280 $mg \cdot kg^{-1}$, which is involved in various plant physiological processes such as chlorophyll synthesis and respiration. Both Mn (94.3 $mg \cdot kg^{-1}$) and Zn (82.8 $mg \cdot kg^{-1}$) were present in considerable amounts, while Cu (17.2 $mg \cdot kg^{-1}$) was relatively low but still required for plant growth. Endowed with diverse and abundant mineral nutrients, *A. annua* has the potential to be converted into mineral nutrient-rich biochar; rational control of key conditions such as temperature and heating rate during the thermochemical conversion stage is expected to achieve the retention and optimization of nutrient forms.

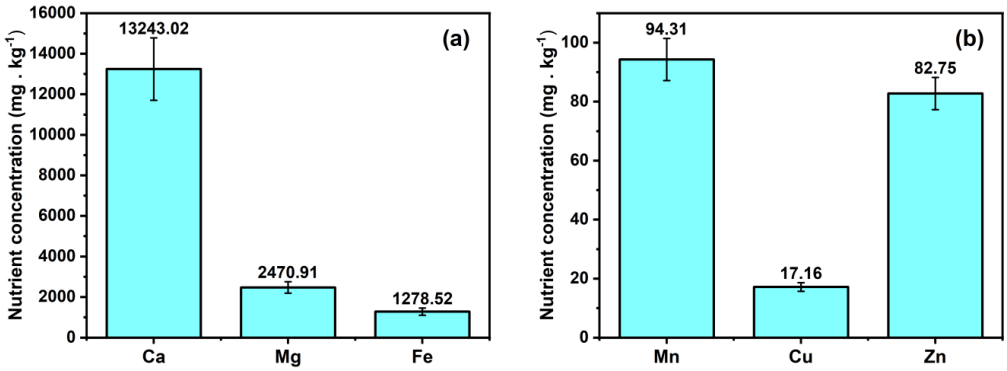

Fig. 1. Concentration of mineral nutrients in *A. annua*

Analysis of Mineral Nutrients in Biochar Prepared by Pyrolysis

Pyrolysis is one of the main technologies for biochar preparation. Its reaction environment of high temperature and oxygen deficiency significantly affects the migration, transformation, and characteristics of mineral nutrients in biochar (Zhou *et al*. 2020).

The concentration of the macroelement Ca in the raw material (Fig. 2a) was 13200 $mg \cdot kg^{-1}$, which was significantly enriched after pyrolysis at 400 ℃ and 500 ℃ (400 ℃: 32700 $mg \cdot kg^{-1}$; 500 ℃: 34600 $mg \cdot kg^{-1}$). This indicates that medium-temperature pyrolysis (400 to 500 ℃) can significantly enhance Ca retention, probably because organic calcium mineralizes to form stable $CaCO_3$ within this temperature range, and the volatilization of organic matter contributes to the relative enrichment of Ca (Huang *et al*. 2024). At 600 ℃, the concentration slightly decreased to 26600 $mg \cdot kg^{-1}$, as $CaCO_3$ thermally decomposes to release CO_2 and convert to CaO, resulting in a reduction in Ca concentration (Zhang *et al*. 2025).

The concentration of the macroelement Mg in the raw material was 2470 $mg \cdot kg^{-1}$ (Fig. 2b). It continued to increase after pyrolysis at 400 and 500 ℃ (400 ℃: 4334.58 $mg \cdot kg^{-1}$; 500 ℃: 5032.5 $mg \cdot kg^{-1}$). This demonstrates that medium-temperature pyrolysis had a superior enrichment effect on Mg, and the removal of easily volatile components such as moisture and organic matter facilitated Mg enrichment. At 600 ℃, the concentration dropped to 3783.33 $mg \cdot kg^{-1}$. MgO generated by the decomposition of $Mg(OH)_2$ at high temperature is prone to volatilization or reaction loss, leading to a significant decrease in Mg concentration (Liu *et al*. 2010).

The concentration of Fe in the raw material was 1280 $mg \cdot kg^{-1}$ (Fig. 2c), which continuously increased with the rise of pyrolysis temperature (400 °C: 2681.25 $mg \cdot kg^{-1}$, 500 °C: 3111.67 $mg \cdot kg^{-1}$, 600 °C: 3250.42 $mg \cdot kg^{-1}$), indicating that pyrolysis promoted Fe retention. This might be due to the decreased loss of Fe chelation caused by organic matter decomposition or the higher stability of mineral Fe (Lian 2021). The concentration of the trace element Mn in the raw material was 94.31 $mg \cdot kg^{-1}$, which gradually increased after pyrolysis (400 ℃: 211 $mg \cdot kg^{-1}$; 500 ℃: 237 $mg \cdot kg^{-1}$) and slightly decreased to 229 $mg \cdot kg^{-1}$ at 600 ℃. During the medium-low temperature stage, the removal of moisture and small-molecule organic matter facilitates the retention of Mn in stable forms (residual fraction, carbonate-bound fraction). At 600 ℃, a small amount of weakly bound Mn (organic-bound fraction, partially unstable carbonate-bound fraction) was slightly decomposed and released, causing a slight fluctuation in concentration, while the overall level still maintains a high enrichment (Zhao *et al*. 2025).

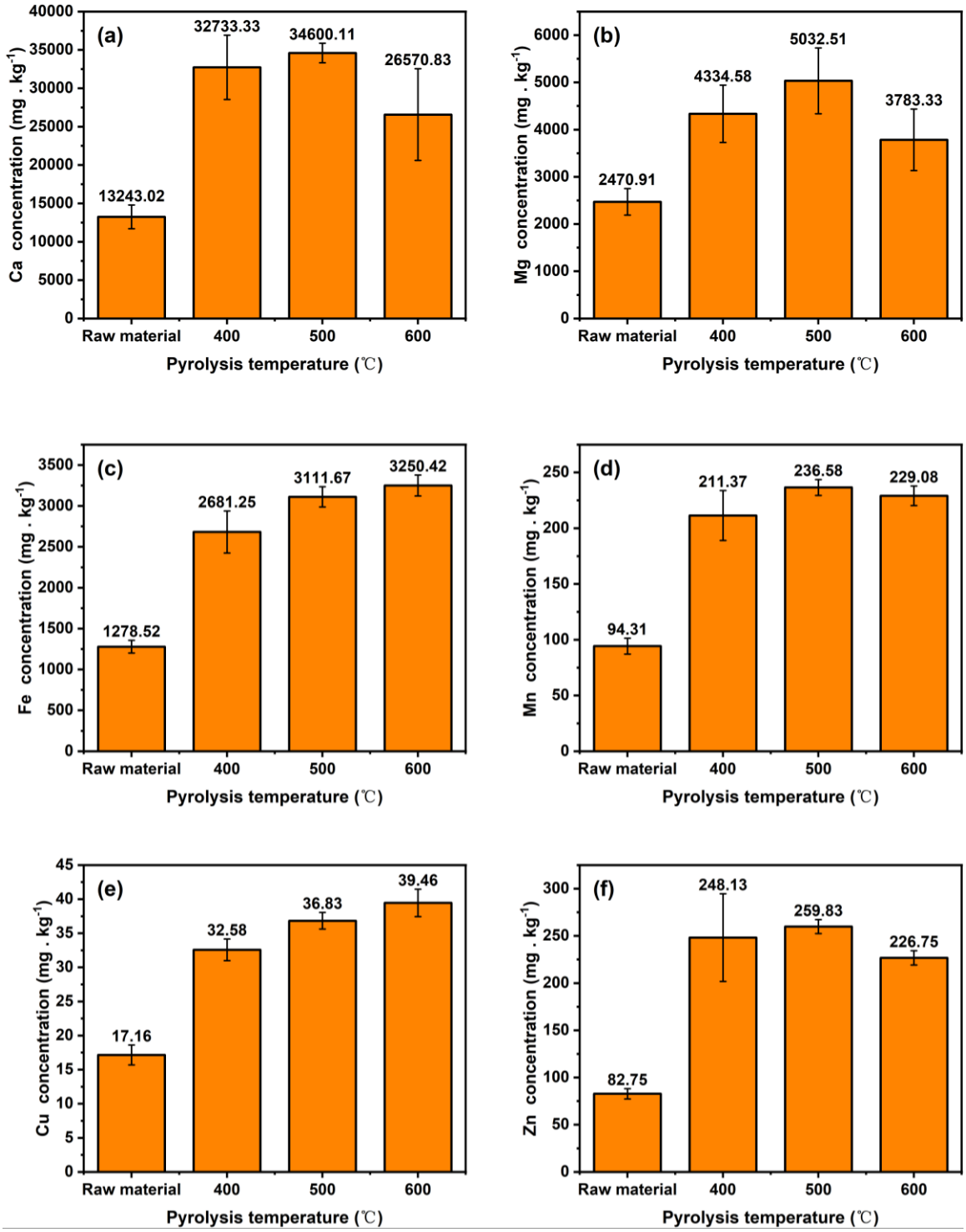

Fig. 2. Concentrations of (a) Ca, (b) Mg, (c) Fe, (d) Mn, (e) Cu, and (f) Zn in *A. annua* biochar prepared by pyrolysis

The concentration of the trace element Cu was 17.2 mg·kg^{-1} (Fig. 2e), which continued to increase along with the temperature rise (400 °C: 32.6 mg·kg^{-1}, 500 °C: 36.8 mg·kg^{-1}, 600 °C: 39.5 mg·kg^{-1}). Pyrolysis is expected to carbonize organic matter, thereby reducing Cu leaching. The higher the temperature, the more significant will be the expected

enrichment (with a gradual slowdown in the increase rate, possibly due to reaching adsorption saturation). The concentration of the trace element Zn was 82.8 mg·kg^{-1} (Fig. 2f), which increased rapidly after pyrolysis at 400 and 500 °C (400 °C: 248.13 mg·kg^{-1}, 500 °C: 260 mg·kg^{-1}) but decreased to 227 mg·kg^{-1} at 600 °C, indicating that moderate-temperature pyrolysis promoted Zn fixation (*e.g.*, binding with surface functional groups of biochar). High temperature might lead to loss due to Zn volatilization (*e.g.*, the sublimation of ZnO at high temperature) (Fan *et al*. 2015).

Analysis of Mineral Nutrients in Biochar Prepared by HTC

HTC is distinguished by its mild medium-temperature and high-pressure liquid reaction environment. It differs significantly from pyrolysis. This water-mediated reaction mechanism endows HTC-derived biochar with distinct mineral nutrient characteristics compared to pyrolytic biochar (Liu *et al*. 2019).

The concentration of the macroelement Ca in the raw material was 13200 mg·kg^{-1} (Fig. 3a), which first increased and then stabilized after HTC (220 ℃: 20500 mg·kg^{-1}; 240 ℃: 18000 mg·kg^{-1}; 260 ℃: 19000 mg·kg^{-1}). Ca was significantly enriched at 220 ℃, probably because its main occurrence forms (*e.g.*, CaC_2O_4, $CaCO_3$) in the low-temperature hydrothermal environment exhibit good thermal stability and are not prone to decomposition and migration. At high temperatures (240 to 260 ℃), part of the weakly bound Ca (unstable organic-bound fraction, a small amount of soluble calcium salts) was leached in the high-temperature and high-pressure aqueous solution, leading to a decrease in concentration that then stabilized (Huang *et al*. 2019).

The macroelement Mg had a concentration of 2470 mg·kg^{-1}. After HTC, its concentration first decreased, then increased (Fig. 3b), decreasing to 1360 mg·kg^{-1} at 220 °C, rising to 1630 mg·kg^{-1} at 240 °C, and greatly increasing to 2650 mg·kg^{-1} at 260 °C. At low temperature (220 °C), Mg was prone to loss with the liquid phase due to its weak binding with biochar functional groups. At high temperature (260 °C), the structural reorganization of biomass allowed more Mg to remain in stable mineral forms (*e.g.*, MgO, $MgCO_3$), thereby achieving enrichment (Zhao *et al*. 2022).

The raw material contained 1280 mg·kg^{-1} of Fe (Fig. 3c), whose concentration increased steadily with rising HTC temperature (220 °C: 2307.51 mg·kg^{-1}; 240 °C: 2890.02 mg·kg^{-1}; 260 °C: 3160.01 mg·kg^{-1}). During the HTC process, decomposition of organic matter reduced chelative loss of Fe, while high temperatures promoted the formation of iron minerals (*e.g.*, Fe_2O_3, Fe_3O_4), enabling more stable enrichment of Fe in biochar (Lian 2021). The Mn concentration was 94.3 mg·kg^{-1} (Fig. 3d), which gradually increased after HTC (220 °C: 138 mg·kg^{-1}; 240 °C: 154 mg·kg^{-1}; 260 °C: 187 mg·kg^{-1}). Higher temperatures deepened biomass carbonization, tightening the binding of Mn with the carbon matrix (*e.g.*, embedding in aromatic ring structures), reducing loss and enhancing enrichment.

For Cu (Fig. 3e), its concentration continuously increased with temperature (220 °C: 29.4 mg·kg^{-1}; 240 °C: 34.0 mg·kg^{-1}; 260 °C: 37.2 mg·kg^{-1}). HTC developed pore structures in biomass and increased surface functional groups, enhancing the adsorption and fixation of Cu^{2+}. Higher temperatures provided more adsorption sites, leading to more significant Cu enrichment. The Zn concentration was 82.8 mg·kg^{-1} (Fig. 3f), which rose rapidly after HTC (220 °C: 151.1 mg·kg^{-1}; 240 °C: 171 mg·kg^{-1}; 260 °C: 230 mg·kg^{-1}). High temperatures promoted chelation of Zn with surface functional groups or formation of stable mineral phases (*e.g.*, ZnO), reducing loss and achieving efficient enrichment.

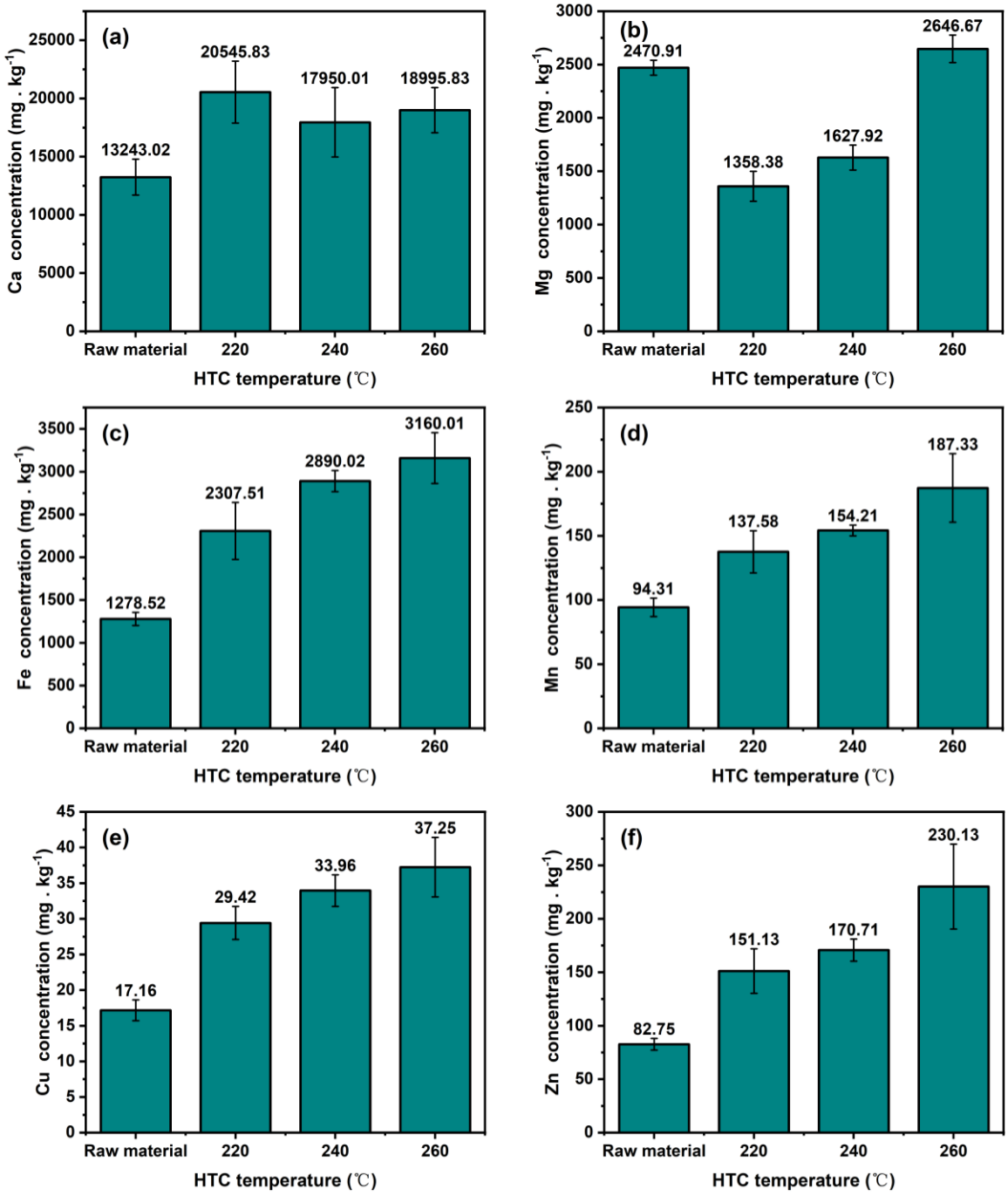

Fig. 3. Concentrations of (a) Ca, (b) Mg, (c) Fe, (d) Mn, (e) Cu, and (f) Zn in *A. annua* biochar prepared by HTC

Yield Analysis of Biochar Prepared under Different Conditions

As shown in Table 1, different thermal conversion processes and temperatures significantly regulated the yield of *A. annua* biochar. In the pyrolysis process (400 to 600 °C), the biochar yield of *A. annua* showed a fluctuating characteristic of first decreasing and then increasing. The yield was 38.3% at 400 °C, decreased to 35.3% at 500 °C, and slightly rebounded to 35.8% at 600 °C. This might be because in the initial stage of pyrolysis (400 to 500 °C), easily decomposable components such as hemicellulose and cellulose in the raw materials were largely pyrolyzed and gasified, leading to a decrease in

yield. When the temperature rose to 600 °C, the carbonization degree of difficult-to-decompose components such as lignin deepened, partial volatile matter might undergo secondary polymerization reactions, increasing the residual amount of solid carbon and causing the yield to recover.

In the HTC process (220 to 260 °C), the yield showed a gradual decreasing trend with increasing temperature, peaking at 220 °C (44.6%), decreasing to 37.2% at 240 °C, further dropping to 36.41% at 260 °C. This pattern originates from the HTC conditions where higher temperatures accelerate the hydrolysis, dissolution, and carbonization of organic matter in raw materials. More small-molecule substances enter the liquid phase, leading to a continuous reduction in the yield of solid biochar.

Table 1. Biochar Yield of *A. annua* under Different Processes

Temperature (°C)	400	500	600	220	240	260
Yield (%)	38.31	35.33	35.84	44.61	37.23	36.41

CONCLUSIONS

1. In *Artemisia annua* biochar prepared by pyrolysis (400 to 600 ℃), Ca and Mg achieved efficient enrichment at 400 to 500 ℃; Mn and Zn reached the optimal enrichment effect with the peak value at 500 ℃, followed by a slight decrease in concentration at 600 ℃. Fe and Cu continuously enriched with increasing pyrolysis temperature, and high temperature enhanced the enrichment more significantly.
2. In *A. annua* biochar prepared by HTC (220 to 260 ℃), Ca was enriched at 220 ℃, and its concentration decreased and stabilized at 240 to 260 ℃. Mg followed a trend of initial loss and subsequent enrichment, realizing efficient enrichment at 260 ℃. The enrichment effects of Fe, Mn, Cu, and Zn were continuously enhanced with the increase of hydrothermal temperature.
3. A comparison of yields showed that: the yield of HTC biochar decreased with increasing temperature, with the maximum yield at 220 ℃; the yield of pyrolysis biochar was slightly lower than that of HTC biochar, which reached the maximum value at 400 ℃, decreased at 500 ℃, and slightly recovered at 600 ℃.

ACKNOWLEDGMENTS

This work was financially supported by Fundamental Research Program of Shanxi Province (No.202403021212115), Research Project Supported by Shanxi Scholarship Council of China (No.2024-124), Doctoral Research Initiation Fund of Taiyuan University of Science and Technology (No.20242051), Taiyuan University of Science and Technology rewarded funds for excellent doctors working in Shanxi Province (No.20242124). 2025 Guangxi University Young and middle-aged teachers' scientific research basic ability improvement project (NO. 2025KY0575); High level Talents Project in Youjiang Medical University for Nationalities (NO. RZ2400001367).

REFERENCES CITED

Fan, S. S., Tang, J., Cheng, Y., Wang, Y., Wang, Z., Tang, J., and Li, X. D. (2015). "Speciation distribution and potential ecological risk of heavy metals in sludge-based biochar," *Ecology and Environmental Sciences* 24(10), 1739-1744. https://doi.org/10.16258/j.cnki.1674-5906.2015.10.022

Huang, N., Lei, M., Wang, H., and Zhao, P. T. (2019). "Co-hydrothermal dealkalization process of high-alkali pine sawdust and high-chlorine waste," *Journal of Engineering Thermophysics* 40(3), 706-715.

Huang, R. X., Nicholas, S., and Wei, Z. (2024). "Thermochemical transformation of calcium during biomass burning and the effects on postfire aqueous dissolution of macronutrients," *Environmental Science & Technology*, 58, 39, 17304-17312. https://doi.org/10.1021/ACS.EST.4C04820

Kou, B. (2023). *Study on Kitchen Waste Compost enhancing Phytoremediation of Cadmium (Cd) in Coal Gangue Piles*, Master's Thesis, Xi'an Shiyou University, Xi'an, China.

Li, F. Z., Teng, Y. T., Zhang, Y. P., and Liu, Y. (2018). "Research status and prospects of disposal technologies for soil heavy metal remediation plants," *Environmental Science & Technology* 41(S2), 213-220.

Li, J. K., Qiu, C. S., Zhao, J. Q., Wang, C. C., Liu, N. N., Wang, D., Wang, S. P., and Sun, L. P. (2023). "Characteristics of biochar prepared from different crop straw raw materials and heavy metal leaching behavior," *Environmental Science* 44(1), 540-548.

Lian, C. (2021). "Study on the adsorption characteristics of biomass pyrolysis/ hydrothermal carbon for pollutants in water," *Master's Thesis*, South China Agricultural University, Guangzhou, China. https://doi.org/10.27152/d.cnki.ghanu.2021.000319

Liu, T., Ma, P. C., Yu, J. K., Li, L., Liu, X. M., and Ma, B. Y. (2010). "Preparation of activated magnesium oxide by thermal decomposition of magnesium hydroxide," *Journal of the Chinese Ceramic Society* 38(7), 1337-1340. https://doi.org/10.14062/j.issn.0454-5648.2010.07.008

Liu, W. (2025). "Application analysis of disposal technologies for historically left-over heavy metal-containing waste residues," *China Resources Comprehensive Utilization* 43(05), 171-173.

Liu, Y. B., and Li, S. Q. (2020). "Characteristics of herbaceous plant communities under different vegetations in reclaimed land of coal gangue hills in Lu'an Mining Area," *Chinese Journal of Applied and Environmental Biology* 26(6), 1392-1399. https://doi.org/10.19675/j.cnki.1006-687x.2019.10041

Liu, Y. T., Wei, J., and Li, J. (2019). "Progress in hydrothermal carbonization of waste biomass and application of its products in wastewater treatment," *Chemistry & Bioengineering* 36(01), 1-10.

Nong, L. X. (2023). "Study on stabilization treatment of heavy metals in hazardous waste incineration fly ash," *China Resources Comprehensive Utilization* 41(12), 216-218.

Shi, Y., Li, J. H., Yu, Y., Yang, Y. W., Li, B., Chen, S. Q., Chen, J., Zao, K., and Huang, J. (2022). "Progress and prospects of combined application of phytoremediation technology with other technologies for heavy metal-contaminated soil," *Environmental Pollution and Control* 44(02), 244-250.

Song, H. J. (2023). *Incineration Characteristics of Heavy Metal-Rich Biomass and*

Resource Utilization of its Products, Ph.D. Dissertation, Hunan Agricultural University, Changsha, China.

Tao, L., Han, X. X., Ren, H. R., Wang, M., Sun, X. N., Wang, R. A., and Ren, J. (2023). "Effects of mineral-modified sludge biochar on soil heavy metal leaching," *Environmental Science & Technology* 46(9), 95-101. https://doi.org/10.19672/j.cnki.1003-6504.0782.23.338

Wang, P. (2019). "Comprehensive analysis of loess slope stability in Bofang Mining Area," *Shandong Coal Science and Technology* 2019(9), 203-205+207.

Xing, J. (2021). *Optimization of Sludge-Based Biochar Preparation and its Remediation of Heavy Metal-Contaminated Soil*, Ph.D. Dissertation, Harbin Institute of Technology, Harbin, China.

Zhang, J. N., Zhang, X. X., Sun, H. F., Wang, C., Liu, S. L., Pu, J. J., and Zhou, S. (2023). "Research status and prospects of biochar-based fertilizers under the 'double carbon' background," *Journal of Zhejiang Agricultural Sciences* 64(12), 2825-2830.

Zhang, X., Zhou, A. G., Gan, Y. Q., Chen, Z. H., and Wang, X. (2010). "Progress in bioremediation of heavy metal-contaminated soils in metal mines," *Environmental Science & Technology* 33(03), 106-112. https://doi.org/10.3969/j.issn.1003-6504.2010.03.024

Zhang, Z. H., Cheng, L., Hu, Q. X., and Hu, Z. Q. (2025). "Influence of pyrolysis temperature on speciation, leaching and environmental risk assessment of heavy metals in biochar and bio-oil from pyrolysis of wet sewage sludge," *Biomass Conversion and Biorefinery* 15(12), 1-14. https://doi.org/10.1007/S13399-025-06530-8

Zhao, H. Y., Wang, Y. L., Shi, T. J., Liu, J. Y., Liu, Y. J., Chen, Y. J., Zhang, R., Wang, Q. H., Chen, Y., Zhu, Y. B., *et al.* (2022). "Ammonium chloride-assisted hydrothermal synthesis of anhydrous magnesium carbonate from magnesium carbonate trihydrate and its formation mechanism," *China Powder Science and Technology* 28(6), 49-57. https://doi.org/10.13732/j.issn.1008-5548.2022.06.006

Zhao, J. Q., Huang, Y. J., Li, Z. Y., Zhu, Z. C., Qi, S. J., Gao, J. W., Liu, J, and Zhang, Y. Y. (2025). "Migration and transformation characteristics of heavy metals during co-pyrolysis of sludge and agricultural-forestry wastes," *Chemical Industry and Engineering Progress* 44(2), 1064-1075. https://doi.org/10.16085/j.issn.1000-6613.2024-0121

Zhou, H. H., Yuan, X. Y., Xiong, Y. T., Han, N., Ye, H. M., and Chen, Y. Z. (2020). "Effects of biochar input on changes in available forms of soil nutrient elements in different riparian zones," *Environmental Science* 41(02), 914-921. https://doi.org/10.13227/j.hjkx.201909006

Article submitted: July 10, 2025; Peer review completed: October 25, 2025; Revised version received: November 22, 2025; Accepted: November 24, 2025; Published: December 3, 2025.
DOI: 10.15376/biores.21.1.570-579